

IRSTI 30.17.35; 27.35.45; 44.31.00

DOI: <https://doi.org/10.26577/JMMCS1302202610>

A. Kereikulova^{1,2} , A. Abdidin¹ , A. Seitov^{1,2} , A. Toleukhanov² , Ye. Belyayev^{1,2*} , O. Botella³ , A. Kheiri³ , M. Khalij³ 

¹Department of Mechanics, Farabi University, Almaty, Kazakhstan
²Department of Mechanical Engineering, Satbayev University, Almaty, Kazakhstan
³CNRS, LEMTA, Universite de Lorraine, Nancy, France
*e-mail: yerzhan.belyayev@gmail.com

NUMERICAL STUDY OF THE EFFECT OF INLET CONFIGURATION AND TANK ORIENTATION ON STRATIFICATION IN A THERMAL ENERGY STORAGE SYSTEM

Thermal energy storage (TES) is a technology that is well established in the solar energy sector, district heating and industrial waste heat recovery. The efficiency of these systems is mostly dependent on the quality of the thermal stratification — the maintenance of a stable temperature difference between the warm and cold section of the tank. Computational fluid dynamics (CFD) techniques are employed to analyze the effects of the inlet configuration and the tank orientation on the charging process of a TES system in this work. A cylindrical tank with height of 1.1 m and inner diameter of 0.46 m is considered with 13 tubes inside the tank to be used in the future for the integration of phase change material (PCM). There are two forms of inlet configuration compared, a distributed shower type inlet and concentrated single orifice, for both vertical and horizontal tank orientations. The numerical model is based on the three-dimensional transient conservation equations for mass, momentum and energy with a variable density of the heat transfer fluid which is a function of temperature. Each configuration is analyzed by the following performance criteria: MIX number, stratification number, storage capacity ratio, and exergy efficiency. The results demonstrate that there is a significant increase in capacity ratio, around 88.5% and exergy efficiency above 88% for vertical configuration compared to horizontal configuration which is reduced to 75–77% and 67–69%, respectively. Shower type inlet produces greater stratification for the vertical orientation due to lesser momentum of the jet than the other inlet design, but it will not have a major impact when compared to tank orientation.

Keywords: thermal energy storage, thermal stratification, CFD, inlet configuration, tank orientation, exergy efficiency.

A. Керейкулова^{1,2}, А. Абдидин¹, А. Сейтов^{1,2}, А. Толеуханов², Е. Беляев^{1,2*}, О. Ботелла³, А. Хейри³, М. Халидж³

¹әл-Фараби атындағы Қазақ ұлттық университеті, Алматы, Қазақстан
²Сәтбаев университеті, Алматы, Қазақстан
³CNRS, LEMTA, Лотарингия университеті, Нанси, Франция
*e-mail: yerzhan.belyayev@gmail.com

Жылу сақтау жүйесіндегі стратификацияға кіріс конфигурациясы мен резервуар орналасу бағытының әсерін сандық зерттеу

Жылу энергиясын сақтау технологиясы (TES) күн энергетикасында, орталықтандырылған жылумен жабдықтау жүйелерінде және өндірістік қалдық жылуды қайта пайдалануда кеңінен қолданылады. Мұндай жүйелердің тиімділігі көбінесе жылулық стратификациясының арқасында, яғни резервуардың ыстық және суық аймақтары арасындағы тұрақты температура айырмасын сақтауға тәуелді. Бұл жұмыста есептеу гидродинамикасы (CFD) әдістері TES жүйесін зарядтау процесіне кіріс конфигурациясы мен резервуардың орналасу бағытының әсерін талдау үшін қолданылған. Биіктігі 1,1 м және ішкі диаметрі 0,46 м болатын

цилиндрлік резервуар қарастырылған. Резервуар ішінде болашақта фазалық ауысу материалы (PCM) енгізілетін 13 түтік орналасқан. Кіріс конфигурациясының екі түрі салыстырылған: таралған душ тәрізді кіріс және бір тесікті кіріс. Бұл салыстыру резервуардың тік және көлденең орналасу жағдайлары үшін жүргізілген. Сандық модель масса, импульс және энергияның үшөлшемді уақытқа тәуелді сақтау теңдеулеріне негізделген. Мұнда жылутасымалдағыштың тығыздығы температураға тәуелді айнымалы шама ретінде алынған. Әрбір конфигурация келесі тиімділік критерийлері бойынша талданған: MIX саны, стратификация саны, жылу сақтау сыйымдылығының коэффициенті және эксергиялық тиімділік. Нәтижелер тік конфигурацияда жылу сақтау сыйымдылығы коэффициентінің шамамен 88.5%-ға дейін жететінің және эксергиялық тиімділіктің 88%-дан жоғары болатынын көрсетті. Ал көлденең конфигурацияда бұл көрсеткіштер сәйкесінше 75–77% және 67–69% дейін төмендейді. Душ тәрізді кіріс тік орналасу жағдайында ағын импульсінің төмен болуына байланысты басқа кіріс түрімен салыстырғанда жақсырақ стратификацияны қамтамасыз етеді. Алайда оның әсері резервуардың орналасу бағытының әсерімен салыстырғанда үлкен емес.

Түйін сөздер: жылу сақтау, жылудық стратификация, CFD, кіріс конфигурациясы, резервуар бағыты, эксергиялық тиімділік.

А. Керейкулова^{1,2}, А. Абдин¹, А. Сейтов^{1,2}, А. Толеуханов², Е. Беляев^{1,2*}, О. Ботелла³, А. Хейри³, М. Халидж³

¹Казахский национальный университет им. аль-Фараби, Алматы, Казахстан

²Satbayev University, Алматы, Казахстан

³CNRS, LEMTA, Университет Лотарингии, Нанси, Франция

*e-mail: yezhan.belyayev@gmail.com

Численное исследование влияния входной конфигурации и ориентации резервуара на стратификацию в системе аккумулирования тепла

Технология хранения тепловой энергии (TES) хорошо зарекомендовала себя в солнечной энергетике, системах централизованного теплоснабжения и утилизации промышленного отходящего тепла. Эффективность таких систем в значительной степени зависит от качества тепловой стратификации — поддержания стабильной разницы температур между горячей и холодной зонами резервуара. В данной работе методы вычислительной гидродинамики (CFD) используются для анализа влияния входной конфигурации и ориентации резервуара на процесс зарядки системы TES. Рассматривается цилиндрический резервуар высотой 1,1 м и внутренним диаметром 0,46 м, внутри которого расположены 13 труб, предназначенных в будущем для интеграции материала с фазовым переходом (PCM). Сравняются два типа входной конфигурации: распределённый душевой вход и концентрированное одиночное отверстие, как для вертикальной, так и для горизонтальной ориентации резервуара. Численная модель основана на трёхмерных нестационарных уравнениях сохранения массы, импульса и энергии с переменной плотностью теплоносителя, зависящей от температуры. Каждая конфигурация анализируется по следующим критериям эффективности: число MIX, число стратификации, коэффициент ёмкости хранения и эксергетическая эффективность. Результаты показывают, что для вертикальной конфигурации наблюдается значительный результат по коэффициенту ёмкости — около 88.5%, а эксергетическая эффективность превышает 88%, тогда как для горизонтальной конфигурации эти показатели снижаются до 75–77% и 67–69%, соответственно. Вход душевого типа для вертикальной ориентации резервуара обеспечивает лучшую стратификацию благодаря меньшему импульсу струи по сравнению с другой конструкцией входа, однако его влияние не столь существенно по сравнению с влиянием ориентации резервуара.

Ключевые слова: тепловое аккумулирование, тепловая стратификация, CFD, входная конфигурация, ориентация резервуара, эксергетическая эффективность.

1 Introduction

Thermal energy storage (TES) systems are used in renewable energy, waste heat recovery, and thermal management applications [1–4]. Sensible heat storage is one of the simplest TES methods because the system design is less complicated and the operating cost is lower compared to other storage technologies. The efficiency of these systems depends on thermal stratification inside the storage tank. A thermocline separates the hot and cold fluid regions. Stable temperature layers reduce thermal losses and improve storage performance [4–6]. It has also been shown that thermocline stability plays a key role in the charging and discharging dynamics of large-scale TES systems [18]. However, inlet jets and fluid circulation inside the tank can disturb the thermal layers and increase mixing. Previous studies investigated the influence of inlet geometry and tank design on thermal stratification. Different inlet configurations such as manifolds, diffuser plates, slotted inlets, and shower-type inlets were proposed to decrease jet penetration and reduce local mixing inside the tank. Distributed inlet systems usually create weaker recirculation regions compared to concentrated inlet designs [7–10]. CFD simulations are widely applied for the analysis of buoyancy-driven flow and heat transfer in TES systems [11, 12]. Studies showed that inlet geometry and tank orientation influence thermocline thickness, thermal plume formation, and charging behaviour. Vertical tanks usually maintain more stable thermal layers because buoyancy forces support the temperature gradient. Horizontal tanks often develop larger recirculation zones and stronger fluid mixing [13, 17]. Additionally, recent studies on thermal energy storage systems [14, 15] have investigated configurations incorporating immersed heat exchangers and PCM containers. These internal components significantly influence the local fluid flow behavior and charging dynamics within the thermal storage tank. In the present study, cylindrical tubes with an inner diameter of 0.04 m were installed inside the thermal energy storage tank, with the intention of subsequently filling these tubes with PCMs. Previous studies [16] investigated the influence of inlet and outlet geometrical configurations, as well as heat transfer fluid flow velocity, on the thermal performance of thermal energy storage (TES) tanks. According to the problem formulation presented in [16], a thermal storage tank designed for high-temperature heat storage was considered, where thermal oil was used as the working fluid and the storage tank did not contain any internal components. In contrast to that study, the present work considers water as the working fluid for domestic thermal energy storage applications and incorporates internal containers to investigate the flow dynamics and thermal performance in the presence of internal elements. The novelty of the proposed research lies in the combined investigation of the inlet geometry and tank orientation effects on the thermal and hydrodynamic behavior of the TES system [16, 17]. In the present study, the charging process of thermal energy storage tanks is investigated using a system of unsteady 3D Navier–Stokes equations with the corresponding initial and boundary conditions. Two inlet and outlet geometrical configurations are considered: the first configuration consists of a single opening positioned above each cylindrical container, while the second configuration employs multiple small openings above each container. In addition, both horizontal and vertical orientations of the main cylindrical storage tanks are analyzed. The primary key performance indicators (KPIs) used to evaluate the thermal performance include the MIX number, stratification number, storage capacity ratio, and exergy efficiency [19–21]. For the numerical implementation of the mathematical model, CFD methods based on the ANSYS

Fluent software package were employed.

2 Materials and Methods

The present work investigates the effect of inlet geometry and tank orientation on thermal stratification during the charging process in a TES system. The main goal is to analyse fluid mixing, thermal behaviour, and exergy efficiency for different configurations. The TES system consists of a cylindrical tank with a height of 1.1 m and an inner diameter of 0.46 m. Inside the tank, 13 cylindrical tubes are installed. Each tube has a length of 1 m and a diameter of 0.04 m. In the numerical model, the tubes are treated as adiabatic internal structures. Heat transfer between the fluid and tube walls is neglected. The tubes mainly affect local flow behaviour and fluid mixing inside the tank. The geometry is also suitable for possible future PCM integration. Water is used as the working fluid in all simulated cases. Initially, the tank is filled with water at 20°C. During charging, hot water at 80°C enters through the inlet section. The charging process continues until the temperature near the bottom region reaches 75°C. A constant volumetric flow rate of 0.0004085 m³/s is applied for all configurations. Two inlet geometries are investigated. The first configuration is a shower-type inlet with eight circular openings per tube (Fig. 1a,c). Each opening has a diameter of 0.01 m. Because the flow enters through several holes, the inlet jet momentum becomes lower and local mixing near the inlet region decreases. The second configuration is a single-orifice inlet with one circular opening per tube and a diameter of 0.027 m (Fig. 1b,d). In this case, the inlet jet becomes more concentrated and stronger local mixing appears. Both inlet geometries are analysed for vertical (Fig. 1a,b) and horizontal (Fig. 1c,d) tank orientations. The vertical tank is used as the reference case because buoyancy helps maintain stable thermal layers. The horizontal orientation is used to analyse the effect of gravity direction on recirculation zones, fluid mixing, and thermocline development. To reduce computational cost, symmetry boundary conditions are applied. A one-quarter three-dimensional model is used for the vertical tank, while a one-half model is used for the horizontal tank. However, all simulations remain fully three-dimensional. Natural convection is considered in the simulations because buoyancy strongly affects thermal stratification inside the tank. Temperature-dependent density variations are calculated using the Boussinesq approximation. Several parameters are used to compare the investigated cases, including the MIX number, stratification number, storage capacity ratio, and exergy efficiency [19]. These parameters are used to evaluate fluid mixing, thermal stratification, and charging performance.

2.1 Governing Equations

The hydrodynamics within a thermal storage tank is simulated by solving three-dimensional, time-accurate balance equations of mass, momentum, and energy. The flow is incompressible and density variations are only accounted for in the gravitational body force term of the momentum equation. The continuity equation is given by:

$$\nabla \cdot \vec{u} = 0 \tag{1}$$

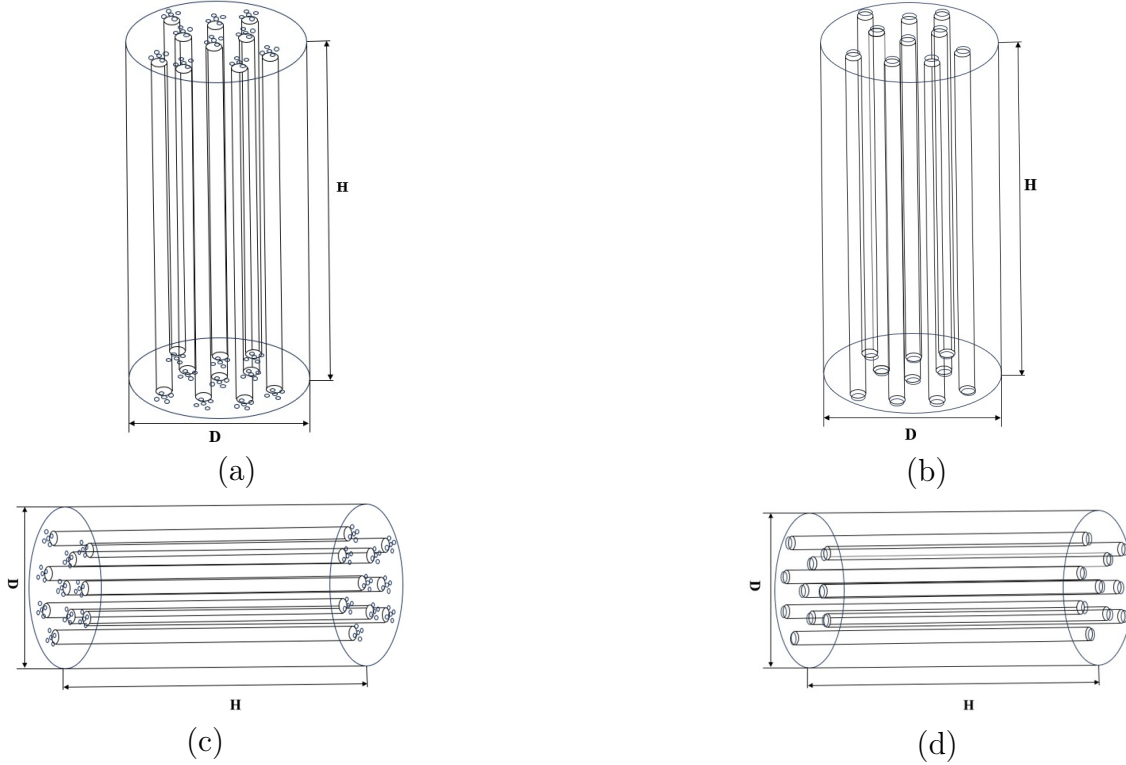


Figure 1: Geometry of the thermal energy storage tank with internal tubes.

The momentum equation is expressed as:

$$\text{x-direction: } \rho \left(\frac{\partial u}{\partial t} + u \frac{\partial u}{\partial x} + v \frac{\partial u}{\partial y} + w \frac{\partial u}{\partial z} \right) = -\frac{\partial p}{\partial x} + \mu \nabla^2 u \quad (2)$$

$$\text{y-direction: } \rho \left(\frac{\partial v}{\partial t} + u \frac{\partial v}{\partial x} + v \frac{\partial v}{\partial y} + w \frac{\partial v}{\partial z} \right) = -\frac{\partial p}{\partial y} + \mu \nabla^2 v \quad (3)$$

$$\text{z-direction: } \rho \left(\frac{\partial w}{\partial t} + u \frac{\partial w}{\partial x} + v \frac{\partial w}{\partial y} + w \frac{\partial w}{\partial z} \right) = -\frac{\partial p}{\partial z} + \mu \nabla^2 w - \rho g \quad (4)$$

where gravity is applied along the negative z-direction (in vertical case $\vec{g} = (0, 0, -g)$, in horizontal case $\vec{g} = (0, -g, 0)$), where the density is a function of temperature, enabling the modeling of natural convection effects. The energy equation governing heat transfer in the fluid is written as:

$$\rho c_p \left(\frac{\partial T}{\partial t} + u \frac{\partial T}{\partial x} + v \frac{\partial T}{\partial y} + w \frac{\partial T}{\partial z} \right) = k \left(\frac{\partial^2 T}{\partial x^2} + \frac{\partial^2 T}{\partial y^2} + \frac{\partial^2 T}{\partial z^2} \right) \quad (5)$$

where \vec{u} is the velocity vector, p is the pressure, T is the temperature, ρ is the temperature-dependent density, c_p is the specific heat capacity, μ is the dynamic viscosity, k is the thermal conductivity, and \vec{g} is the gravitational acceleration vector.

The density of water is modeled using the Boussinesq approximation, assuming a linear variation with temperature:

$$\rho = \rho_{ref} [1 - \beta(T - T_{ref})] \quad (6)$$

where ρ_{ref} is the density at the reference temperature T_{ref} , and β is the thermal expansion coefficient. This formulation enables the incorporation of buoyancy effects while neglecting density variations in all terms except the gravitational body force. For comparison purposes, an additional temperature-dependent density formulation was also implemented through a user-defined function (UDF) using a polynomial approximation:

$$\rho(T_c) = \sum_{i=0}^5 a_i T_c^i \quad (7)$$

where T_c is the temperature, and a_i are polynomial coefficients obtained from established correlations for water thermophysical properties [22]. Simulations comparing the Boussinesq approximation (6) and UDF-based density model (7) showed little difference between the two in terms of thermal and flow behavior for these test operating conditions. Subsequent simulations utilized the Boussinesq approximation due to computational efficiency advantages.

Table 1 summarises the dimensionless parameters used for describing the flow behaviour in the investigated configurations together with their physical interpretation and corresponding value ranges.

The results show that natural convection dominates over forced convection in all analysed cases. The flow remains laminar and the Mach number stays low during the simulations. Therefore, the flow can be considered incompressible. All solid surfaces are treated as no-slip walls. The tank walls are assumed to be adiabatic, so heat losses to the surroundings are neglected. Transient simulations are used to study thermocline development and thermal stratification during charging. To validate the mathematical and numerical models presented in this study, a comparison was conducted with experimental data available in the open literature.

The numerical results were compared with the experimental data reported by Zachar et al. [8]. Good agreement between the numerical and experimental temperature profiles was obtained, with a mean absolute error (MAE) of 1.12% and a root mean square error (RMSE) of 2.03%. These results confirm the applicability and reliability of the proposed CFD model for the investigation of thermal stratification phenomena in TES systems [16]. The validation results confirm the applicability and reliability of the proposed numerical tool for investigating various configurations of thermal energy storage tanks.

3 Results and Discussion

A mesh independence assessment was performed for all investigated configurations in order to ensure numerical accuracy and solution stability. The mesh size for all cases was maintained within the range of 0.008–0.01 m. For the configurations with multiple inlet openings above the cylindrical containers, the computational mesh consisted of approximately 85,790 nodes and 436,762 elements. For the configurations with a single inlet opening above

Table 1: Dimensionless analysis of inlet configurations and tank orientations

Parameter	Shower Vertical	Orifice Vertical	Shower Horizontal	Orifice Horizontal	Interpretation
Height (m)	1.1	1.1	0.46	0.46	Governs buoyancy strength
Velocity (m/s)	0.05	0.055	0.05	0.055	Slightly higher in orifice cases
Reynolds number (Re)	500	1510	500	1510	Laminar flow, $Re < 2300$
Mach number (Ma)	$3.3 \cdot 10^{-5}$	$3.7 \cdot 10^{-5}$	$3.3 \cdot 10^{-5}$	$3.7 \cdot 10^{-5}$	Low Mach number for all cases (incompressible flow), $Ma < 0.3$
Peclet number (Pe)	3500	10500	3500	10500	Convective heat transfer dominates, $Pe \gg 1$
Rayleigh number (Ra)	$2.5 \cdot 10^{12}$	$2.5 \cdot 10^{12}$	$1.8 \cdot 10^{11}$	$1.8 \cdot 10^{11}$	Strong buoyancy effects
Grashof number (Gr)	$3.5 \cdot 10^{11}$	$3.5 \cdot 10^{11}$	$2.5 \cdot 10^{10}$	$2.5 \cdot 10^{10}$	Natural convection dominates
Richardson number (Ri)	$1.4 \cdot 10^6$	$1.5 \cdot 10^5$	10^5	10^4	Buoyancy dominates inertia
Number of holes	104	13	104	13	Defines jet distribution and mixing

the cylindrical containers, the mesh contained approximately 85,139 nodes and 434,270 elements. The mesh quality was evaluated using standard numerical quality indicators. The skewness values remained below 0.83 (recommended value < 0.85), the aspect ratio was within the range of 8–9 (recommended range 10–20), and the orthogonal quality remained above 0.25 (recommended value > 0.1 –0.2). Based on these indicators, the generated computational meshes were considered suitable for the present CFD simulations. Detailed mesh quality evaluation procedures and validation analyses were previously reported in the authors' earlier work [16]. For the thermal energy storage tank configurations described above, Figure 2 presents the temperature contour distributions during the charging process at time intervals of 180 s and 420 s. Figures 2(a) and 2(b) illustrate the vertical storage tank configurations with a single opening above the internal cylindrical containers and with multiple openings, respectively. Meanwhile, Figures 2(c) and 2(d) present the corresponding results for the horizontal orientation of the main external storage tank. According to the obtained results, it can be observed that for the vertical orientation of the external storage tank, the hot and cold water regions become clearly separated approximately 180 s after the beginning of the charging process. The numerical tool accurately captures the physical flow behavior,

as evidenced by the fact that the hot water remains predominantly in the upper region of the tank, while the colder water is concentrated near the bottom. For the configuration with multiple small inlet openings above the internal cylindrical containers, the thermocline region, or temperature transition zone, appears smoother due to the distributed inflow through several smaller openings. The reduced inlet momentum decreases local mixing effects near the inlet region. In contrast, for the configuration with a single jet-type opening above the internal container, the incoming flow becomes more concentrated, leading to stronger localized mixing within the storage tank. As illustrated in Figures 2(c) and 2(d), the horizontal orientation of the storage tanks results in more intensive fluid mixing compared with the vertical configurations. During the initial stage of the charging process, buoyancy forces combined with the primary flow direction generate larger recirculation regions inside the tank. Consequently, the temperature field becomes less stable, and the thermocline region remains thicker. Although thermal stratification still develops during the charging process, the stratified thermal layers are noticeably weaker than those observed in the vertical tank configurations.

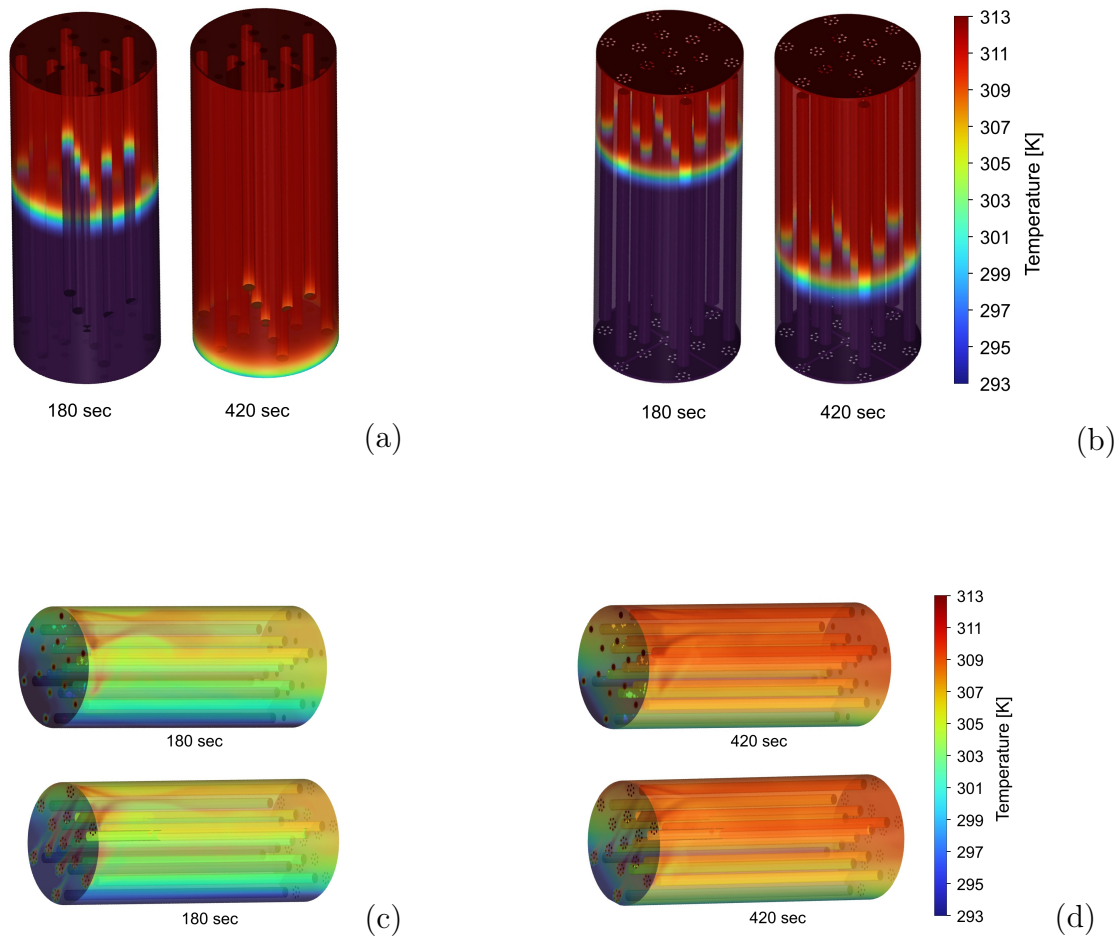


Figure 2: Temperature contours for different inlet configurations and tank orientations. (a) Vertical orifice inlet at 180 s and 420 s, (b) vertical shower inlet at 180 s and 420 s, (c) horizontal tank at 180 s, and (d) horizontal tank at 420 s, including both inlet configurations.

Figure 3 illustrates the average values of the MIX number and stratification number for the above-mentioned storage tank configurations during the charging process. For the vertical tank orientations, the MIX number does not exceed 0.15 for either inlet condition. In comparison, the stratification number remains close to unity and exhibits a slight increase for the inlet configuration with multiple small openings. Due to the lower inlet momentum, disturbances within the thermal layers are reduced, resulting in improved thermal stratification inside the storage tank. In contrast to the vertical configurations, the horizontal storage tank configurations exhibit different thermal and hydrodynamic characteristics. At the initial stage of the charging process, the MIX number reaches values in the range of approximately 0.4–0.7, which are significantly higher than those observed for the vertical configurations. Conversely, the stratification number exhibits lower values during the early charging period. In horizontal storage tanks, gravitational forces act against the development of the temperature gradient, thereby enhancing fluid circulation and mixing within the reservoir. As the charging process progresses, the temperature field gradually becomes more uniform, while the stratification number correspondingly increases over time.

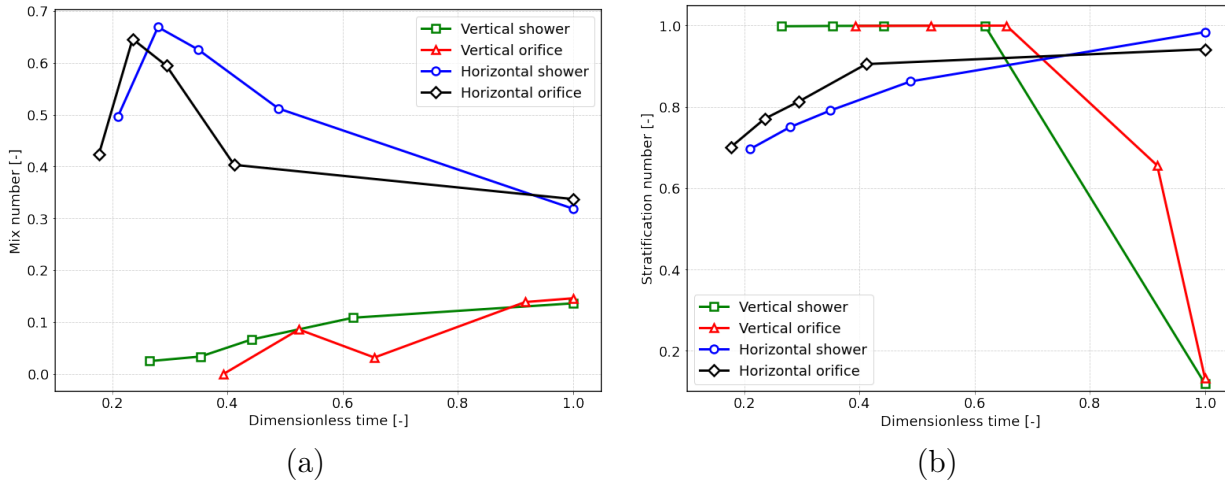


Figure 3: Evolution of (a) MIX number and (b) stratification number as a function of dimensionless charging time for different inlet configurations and tank orientations. Lower MIX values indicate reduced thermal mixing and improved stratification, while stratification numbers closer to unity correspond to better thermocline preservation and TES performance.

Figure 4 presents the key performance indicators evaluated at the end of the charging process, including the storage capacity ratio and exergy efficiency, for all investigated cases. The vertical configurations show better thermal performance compared to the horizontal cases. Stronger mixing inside the horizontal tanks creates a more uniform temperature distribution and reduces storage efficiency. For the horizontal orifice-type configuration, the storage capacity ratio reaches 77.17%, while the exergy efficiency reaches 69.28%. In the horizontal shower case, lower values of 75.53% and 67.30% are obtained. For the horizontal orientation, the orifice inlet performs slightly better than the shower-type inlet. The results show that tank orientation has a larger influence on thermal stratification and TES performance than inlet geometry. The shower-type inlet reduces local mixing because the incoming flow is distributed through several openings. However, tank orientation still

remains the dominant factor for thermal behaviour inside the TES system.

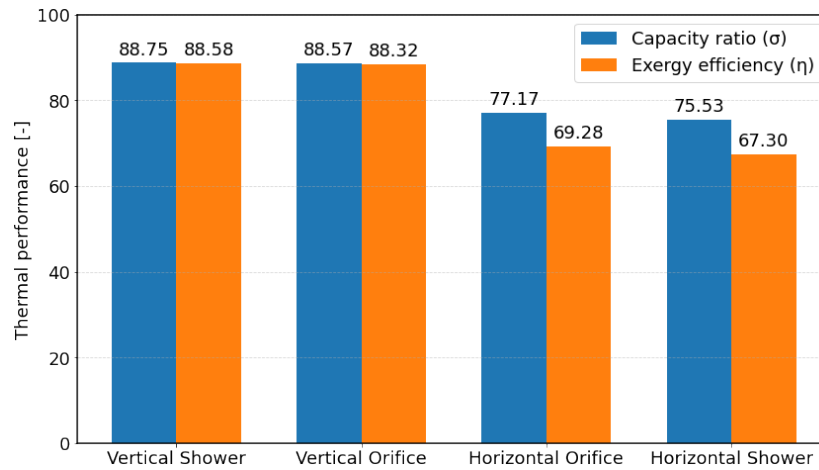


Figure 4: Storage capacity ratio and exergy efficiency for vertical and horizontal thermal energy storage tank configurations with shower-type and orifice inlets at the end of the charging process. The storage capacity ratio represents the effectiveness of useful thermal energy storage within the tank, while exergy efficiency evaluates the quality and thermodynamic usefulness of the stored thermal energy. Higher values of both indicators correspond to improved thermal stratification and reduced irreversible mixing effects inside the TES system.

Conclusion. Transient three-dimensional CFD simulations were carried out for a cylindrical TES system with different inlet geometries and tank orientations. For the vertical configurations, stable thermal layers formed because buoyancy supported the temperature gradient. In the horizontal cases, larger recirculation regions appeared and fluid mixing increased, which weakened thermal stratification. The shower-type inlet showed slightly better stratification behaviour for the vertical orientation because the inlet momentum was lower and local mixing near the inlet region decreased. Still, tank orientation had a larger influence on TES performance than inlet geometry. The vertical configurations also showed higher storage capacity ratios and exergy efficiencies (above 88%). In the horizontal cases, stronger mixing reduced thermal performance and lower efficiency values were obtained. Buoyancy conditions played the main role in thermocline formation and TES performance for all investigated cases.

Acknowledgments. This research is funded by the Committee of Science of the Ministry of Science and Higher Education of the Republic of Kazakhstan under Grant No. AP26100473, “Study of Cascade Solar Thermal Energy Storage Efficiency in Solid-State Heat Storages using Phase Change Materials for Domestic Applications in Continental Climate Conditions”, 2025–2027.

The authors express their sincere gratitude to the “Heat Management” research team at the LEMTA R&D Center of the University of Lorraine and CNRS (Nancy, France) for their valuable support.

The authors also acknowledge the organizers of the double-degree Master’s program between Al-Farabi Kazakh National University (Kazakhstan) and the University of Lorraine (France), specializing in “7M05405 – Mechanics and Energy,” for their contribution to the

academic preparation of Master's graduates.

Nomenclature		Abbreviations	
\vec{u}	velocity vector, m/s	TES	Thermal Energy Storage
u, v, w	velocity components in x, y, z directions, m/s	CFD	Computational Fluid Dynamics
p	pressure, Pa	UDF	User Defined Function
T	temperature, K	PCM	Phase Change Material
T_{ref}	reference temperature, K	HTF	Heat Transfer Fluid
T_c	temperature used in polynomial density correlation, K	KPI	Key Performance Indicator
ρ	density, kg/m ³		
c_p	specific heat capacity, J/(kg·K)		
k	thermal conductivity, W/(m·K)		
μ	dynamic viscosity, Pa·s		
β	thermal expansion coefficient, K ⁻¹		
\vec{g}	gravitational acceleration vector, m/s ²		
a_i	polynomial coefficients		
D	tank diameter, m		
H	tank height, m		
MIX	mixing number, –		
Str	stratification number, –		
η	exergy efficiency, %		
σ	capacity ratio, %		

References

- [1] Zhang, H., J. Baeyens, G. Caceres, J. Degreve, and Y. Lv. "Thermal Energy Storage: Recent Developments and Practical Aspects." *Progress in Energy and Combustion Science* 53 (2016): 1–40.
- [2] Pelay, U., L. Luo, Y. Fan, D. Stitou, and C. Castaing. "Integration of a Thermochemical Energy Storage System in a Rankine Cycle Driven by Concentrating Solar Power: Energy and Exergy Analyses." *Energy* 167 (2019): 498–510.

-
- [3] Pelay, U., L. Luo, Y. Fan, D. Stitou, and M. Rood. "Thermal Energy Storage Systems for Concentrated Solar Power Plants." *Renewable and Sustainable Energy Reviews* 79 (2017): 82–100.
- [4] Li, G. "Sensible Heat Thermal Storage: Energy and Exergy Performance Evaluations." *Renewable and Sustainable Energy Reviews* 53 (2016): 897–923.
- [5] Karim, A., A. Burnett, and S. Fawzia. "Investigation of Stratified Thermal Storage Tank Performance for Heating and Cooling Applications." *Energies* 11 (2018): 1049.
- [6] Altuntop, N., Z. Kilic, V. Ozcelyhan, and O. Kincay. "Effect of Water Inlet Velocity on Thermal Stratification in a Mantled Hot Water Storage Tank." *International Journal of Energy Research* 30 (2006): 163–176.
- [7] Davidson, J. H., and D. A. Adams. "Fabric Stratification Manifolds for Solar Water Heating." *Journal of Solar Energy Engineering* 116 (1994): 130–136.
- [8] Zachar, A., I. Farkas, and F. Szlavka. "Numerical Analyses of the Impact of Plates for Thermal Stratification Inside a Storage Tank with Upper and Lower Inlet Flows." *Solar Energy* 74 (2003): 287–302.
- [9] Li, S.-H., Y.-X. Zhang, Y. Li, and X.-S. Zhang. "Experimental Study of Inlet Structure on the Discharging Performance of a Solar Water Storage Tank." *Energy and Buildings* 70 (2014): 490–496.
- [10] Shah, L. J., and S. Furbo. "Entrance Effects in Solar Storage Tanks." *Solar Energy* 75 (2003): 337–348.
- [11] Shafieian, A., H.-R. Bahrami, A. Roostaei, and S. S. Feyzi. "Effects of Different Inlet Configurations on the Performance of Solar Storage Tanks: A Three-Dimensional Unsteady CFD Simulation." *Case Studies in Thermal Engineering* 45 (2023): 103019.
- [12] Abdidin, A., A. Seitov, A. Toleukhanov, O. Botella, A. Kheiri, and Y. Belyayev. "Three-Dimensional CFD Analysis of a Hot Water Storage Tank with Various Inlet/Outlet Configurations." *Energies* 17 (2024): 5716.
- [13] Abdelhak, O., H. Mhiri, and P. Bournot. "CFD Analysis of Thermal Stratification in Domestic Hot Water Storage Tank During Dynamic Mode." *Building Simulation* 8 (2015): 291–301.
- [14] Caliano, M., N. Bianco, G. Graditi, and L. Mongibello. "Analysis of a Phase Change Material-Based Unit by Numerical Simulation." *Applied Energy* 256 (2019): 113921.
- [15] Liu, G., J.-Y. Zhang, H.-J. Li, Q.-Y. Ji, and Q. Zhou. "Numerical Study on Stratification Performance of Cascaded Three-Layered Packed-Bed in the Thermal Storage Process." *Applied Thermal Engineering* 219 (2023): 119669.
- [16] Kereikulova, A., Y. Yerdesh, Y. Belyayev, A. Toleukhanov, O. Botella, A. Kheiri, and M. Khalij. "Impact of Inlet Configuration and Flow Rates on Thermal Storage Stratification and Efficiency." *Thermo* 6, no. 1 (2026): 16.

- [17] van Schalkwyk, P. D., J. P. Meyer, J. A. A. Engelbrecht, and M. J. Booysen. "Numerical Modelling of Thermal Stratification Scenarios in Horizontal Electric Hot Water Storage Tanks." *Applied Thermal Engineering* 258 (2025): 124716.
- [18] Bayon, R., and E. Rojas. "Simulation of Thermocline Storage for Solar Thermal Power Plants: From Dimensionless Results to Prototypes and Real-Size Tanks." *International Journal of Heat and Mass Transfer* 60 (2013): 713–721.
- [19] Lou, W., L. Luo, Y. Hua, Y. Fan, and Z. Du. "A Review on the Performance Indicators and Influencing Factors for Thermocline Thermal Energy Storage Systems." *Energies* 14 (2021): 8384.
- [20] Jayabal, R., B. Nagappan, S. P. Jena, A. Tiwari, V. Raju K., A. Kushwah, G. Gulothungan, A. Smerat, and K. K. Priya. "Hybrid Solar-PCM Energy Storage Systems: Design Optimization, Thermal Management, Performance Benchmarking, and Techno-Economic Perspectives." *Results in Engineering* (2026): 111193.
- [21] Bielsa, D., P. Arribalzaga, I. Martinez, M. Hashemi-Tilehnoee, I. Torrano, A. Serrano, and E. Palomo del Barrio. "Experimental and Numerical Study of a Novel Cost-Effective Macro-Encapsulated Solid-Solid PCM for Solar Process Heat Thermal Energy Storage." *Applied Thermal Engineering* 280 (2025): 128460.
- [22] Fofonoff, N. P., and R. C. Millard Jr. *Algorithms for Computation of Fundamental Properties of Seawater*. UNESCO Technical Papers in Marine Science 44. Paris: UNESCO, 1983.

Information about authors:

Aiyym Kereikulova – PhD student, Al-Farabi Kazakh National University (Almaty, Kazakhstan, aiymkereikulova56@gmail.com).

Alina Abdidin – Master’s student, Al-Farabi Kazakh National University and University of Lorraine (Almaty, Kazakhstan, alinaa808@gmail.com).

Abzal Seitov – PhD student, Al-Farabi Kazakh National University (Almaty, Kazakhstan, seitov.abz19@gmail.com).

Amankeldy Toleukhanov – PhD, Associate Professor, Satbayev University (Almaty, Kazakhstan, aman.toleukhanov@gmail.com).

Yerzhan Belyayev – PhD, Associate Professor, Al-Farabi Kazakh National University (Almaty, Kazakhstan, yerzhan.belyayev@gmail.com).

Olivier Botella – PhD, Associate Professor, University of Lorraine (Nancy, France, olivier.botella@univ-lorraine.fr).

Abdelhamid Kheiri – PhD, Associate Professor, University of Lorraine (Nancy, France, abdelhamid.kheiri@univ-lorraine.fr).

Mohammed Khalij – PhD, Associate Professor, University of Lorraine (Nancy, France, mohammed.khalij@univ-lorraine.fr).

Авторлар туралы мәлімет:

Керейкулова Айым Есенқұлқызы – әл-Фараби атындағы Қазақ ұлттық университетінің PhD студенті (Алматы, Қазақстан, aiymkereikulova56@gmail.com).

Абдидин Алина Нурлыбекқызы – әл-Фараби атындағы Қазақ ұлттық университеті мен Лотарингия университетінің магистрі (Алматы, Қазақстан, alinaa808@gmail.com).

Сейтов Абзал Ниязбекұлы – әл-Фараби атындағы Қазақ ұлттық университетінің PhD докторанты (Алматы, Қазақстан, seitov.abz19@gmail.com).

Төлеуханов Аманкелді Елешұлы – PhD, Satbayev University қауымдастырылған профессоры (Алматы, Қазақстан, aman.toleukhanov@gmail.com).

Беляев Ержан Келесұлы – PhD, әл-Фараби атындағы Қазақ ұлттық университетінің қауымдастырылған профессоры (Алматы, Қазақстан, yerzhan.belyayev@gmail.com).

Olivier Botella – PhD, University of Lorraine қауымдастырылған профессоры (Нанси, Франция, olivier.botella@univ-lorraine.fr).

Abdelhamid Kheiri – PhD, University of Lorraine қауымдастырылған профессоры (Нанси, Франция, abdelhamid.kheiri@univ-lorraine.fr).

Mohammed Khalij – PhD, University of Lorraine қауымдастырылған профессоры (Нанси, Франция, mohammed.khalij@univ-lorraine.fr).

Сведения об авторах:

Керейкулова Айым Есенкуловна – PhD студент КазНУ им. аль-Фараби (Алматы, Қазақстан, aiutkereiikulova56@gmail.com).

Абдидин Алина Нурлыбековна – магистр КазНУ им. аль-Фараби и Университета Лотарингии (Алматы, Қазақстан, alinaa808@gmail.com).

Сейтов Абзал Ниязбекович – PhD докторант КазНУ им. аль-Фараби (Алматы, Қазақстан, seitov.abz19@gmail.com).

Төлеуханов Аманкелды Елешевич – PhD, ассоциированный профессор Satbayev University (Алматы, Қазақстан, aman.toleukhanov@gmail.com).

Беляев Ержан Келесович – PhD, ассоциированный профессор КазНУ им. аль-Фараби (Алматы, Қазақстан, yerzhan.belyayev@gmail.com).

Olivier Botella – PhD, ассоциированный профессор University of Lorraine (Нанси, Франция, olivier.botella@univ-lorraine.fr).

Abdelhamid Kheiri – PhD, ассоциированный профессор University of Lorraine (Нанси, Франция, abdelhamid.kheiri@univ-lorraine.fr).

Mohammed Khalij – PhD, ассоциированный профессор University of Lorraine (Нанси, Франция, mohammed.khalij@univ-lorraine.fr).

*Revised: May 17, 2026
Accepted: June 15, 2026*